J. Fluid Mech. (2022), *vol*. 933, A52, doi:10.1017/jfm.2021.1103

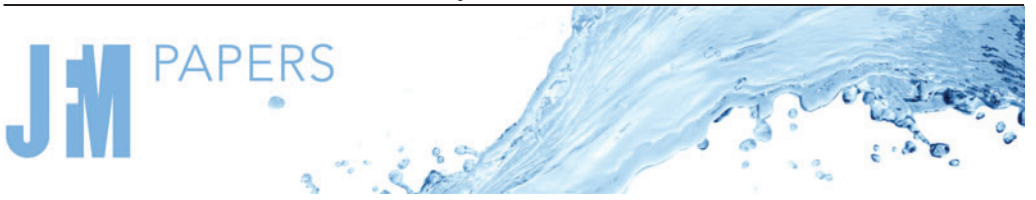

Trapping patterns during capillary displacements in disordered media

Fanli Liu[1] **and Moran Wang**[1],†

[1]Department of Engineering Mechanics, Tsinghua University, Beijing 100084, PR China

(Received 26 August 2021; revised 8 October 2021; accepted 3 December 2021)

We investigate the impact of wettability distribution, pore size distribution and pore geometry on the statistical behaviour of trapping in pore-throat networks during capillary displacement. Through theoretical analyses and numerical simulations, we propose and prove that the trapping patterns, defined as the percentage and distribution of trapped elements, are determined by four dimensionless control parameters. The range of all possible trapping patterns and how the patterns are dependent on the four parameters are obtained. The results help us to understand the impact of wettability and structure on trapping behaviour in disordered media.

Key words: porous media, multiphase flow

1. Introduction

Fluid–fluid immiscible displacements in porous media are important in many fields of industry, such as carbon dioxide storage, and oil recovery and soil infiltration (Berg & Ott 2012; Huppert & Neufeld 2014; Tsuji, Jiang & Christensen 2016; Odier *et al.* 2017; Tran, Neogi & Bai 2017; Vishnudas & Chaudhuri 2017), and one major concern is to increase or decrease trapping of the defending fluid. The fluid invasion process is governed by the viscous force and the capillary force, which depends on flow rate, viscosity, interfacial tension, wettability and porous structure. Interplay between different factors produces different distributions of trapped ganglia size (Avendaño *et al.* 2019; Wang, Pereira & Gan 2020), and displacement patterns ranging from fractal and ramified to compact, when either viscous force (Chen & Wilkinson 1985; Måløy, Feder & Jøssang 1985; Lenormand, Touboul & Zarcone 1988; Aker, Måløy & Hansen 2000; Rabbani *et al.* 2018; Gu, Liu & Wu 2021) or capillary force (Lenormand & Zarcone 1985; Cieplak & Robbins 1988; Lenormand *et al.* 1988; Holtzman & Segre 2015; Trojer, Szulczewski & Juanes 2015) dominates. The purpose of this work is to investigate the statistical behaviour of trapping during capillary displacement. For simplicity, in the following text the invading and

† Email address for correspondence: mrwang@tsinghua.edu.cn

defending fluids are respectively referred to as water and oil. With negligible viscous impact, the governing factors are wettability and structure (Zhao, MacMinn & Juanes 2016), and in the literature (Cieplak & Robbins 1988; Holtzman & Segre 2015; Blunt 2017) it is suggested that a water-wet condition and homogeneous structure produce a compact displacement pattern with the help of a cooperative effect. Yet the interplay between heterogeneous wettability distribution and heterogeneous structure relatively lacks study (Wang *et al.* 2019; Wang, Pereira & Gan 2021), which is of more importance especially when there is wettability alteration (Berg *et al.* 2010; Liu & Wang 2020; Taheriotaghsara *et al.* 2020). In this work, we study the trapping patterns by numerical simulations of water invasion on two-dimensional (2-D) networks of disordered media, which are initially filled with oil, with various wettability distributions and structure to clarify their impacts.

2. Methods

We perform numerical simulations of water invasion on 2-D networks of disordered media, which are initially filled with oil. Under such physical settings, layer flow and snap-off can be ignored (Al-Gharbi & Blunt 2005; Singh *et al.* 2019; Esmaeilzadeh *et al.* 2020). The algorithm follows the idea of pore-network modelling, where the network is viewed as a collection of pores and throats, and the elements (pore or throat) are filled in ascending order of their entry pressure (Blunt 1998; Zhao *et al.* 2019). In the traditional pore-network model, the entry pressure of a throat depends on its size and contact angle as $P_c = \sigma \cos\theta / r$, where σ is the interfacial tension, r is the radius of the element and θ is the contact angle of oil. The entry pressure of a pore additionally depends on the number of connected throats filled with water, namely the cooperative effect, and it is often introduced by a parametric model: $P_c = \sigma \cos\theta / r - \sigma \sum_1^n A_i x_i$, where n is the number of connecting oil-filled throats, x_i are random numbers and A_i are arbitrary parameters (Valvatne & Blunt 2004). We make two modifications in our algorithm. First, we introduce a geometric parameter, the diverging angle ϕ, to capture the inevitable diverging feature at a throat–pore junction (Payatakes 1982) shown in figure 1. This is a simplified treatment for a 2-D structure that has been applied recently in generalized network modelling (Raeini, Bijeljic & Blunt 2018). Second, we propose that the multiple adjacent throats filled with water do not necessarily lead to cooperative pore filling. The relevant pores must be partly filled so that the interface encounters other throats. Therefore we track the interface within pores for more exact description of the cooperative effect. The numerical realization is as follows. We allow pores to be partly filled instead of either filled or unfilled. An unfilled pore has a primary capillary entry pressure Pc_1 that determines whether the interface can advance to contact other throats and become a partly filled pore, and a partly filled pore has a secondary entry pressure Pc_2 that determines whether it can be fully filled. In other words, a pore is now filled in two steps instead of one. More complex topology can lead to more than two steps of pore filling. Inside the diverging channel, $P_c = (\sigma + \phi)\cos\theta / r$, where r is a variable ranging from the radius of the relevant throat and pore, and Pc_1 is the largest of the Pc. Here, Pc_2 depends on the number of cooperative throats, namely throats filled with invading fluid, and touches the interface: $P_c = C_n(\sigma + \phi)\cos\theta / r$; and C_n are coefficients related to structure and can in theory vary for different pores. Two requirements should be met: $C_2 = 1$, meaning that the radius of curvature is the same as the radius of the pore when only one throat is unfilled for cooperative pore filling, a requirement recognized in previous works; and $C_0 > C_1 > C_2$, which is a general geometrical requirement. In this work we use a simple treatment that $C_0 = 2$, $C_1 = 1.4$,

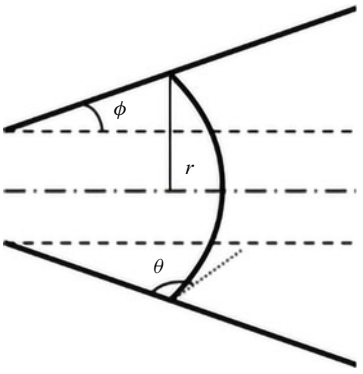

Figure 1. Illustration of the diverging feature at a throat–pore junction. A geometric parameter, diverging angle ϕ, is introduced to capture it. This allows better description of porous structure than in the traditional pore-network model.

$C_2 = 1$. The necessity of such modifications and benchmark for our algorithm are shown in the Appendix.

The topology of networks is fixed throughout this study as a 400×400 square lattice, while distributions of the wettability, the pore size and the geometric parameter are varied. For given distributions, each element is assigned a size, a contact angle and diverging angles in a random and independent way spatially. Trapping occurs when oil is surrounded by water, and every simulation ends when all oil phase is fully trapped. This work cares only about the capillary-dominated trapping process, while the post-trapping oil ganglion dynamics (Rücker *et al.* 2015) will not be considered.

3. Results and discussion

The trapping patterns are summarized by analysing the simulation results. The statistical behaviour of trapping in plain words is how many and what kinds of elements are being trapped. In the model of the present work, each element can be characterized by its entry pressure and its state, a pore or a throat. Therefore the percentage and the distribution of trapped pores and throats along the sequence of their entry pressure fully capture the statistical information, which are defined as the trapping pattern for a given set of distributions (contact angle, pore size and diverging angle). Note that the same set of distributions corresponds to numerous spatially different networks, which may produce different displacing sequences, yet their trapping patterns are proved to be the same statistically, with a standard deviation less than 1 %.

It is noted that the combination of all three distributions yields numerous possibilities and it is unpractical to cover all cases directly. We propose several dimensionless parameters, which can be calculated from the distributions, essentially controlling the trapping pattern, thus all possible trapping patterns can be obtained by varying these parameters. First, we consider the simplified case that the pore filling is negligible and the entry pressure of pores is calculated in the same way as for throats. This makes the model reduce to invasion percolation (IP) with trapping (Wilkinson & Willemsen 1983; Sheppard *et al.* 1999; Sahini & Sahimi 2003). It is recognized that the hierarchy of entry pressures instead of the absolute value actually determines the result of IP, which is equivalent to knowing the order relation between any two elements. We further note that when an element is adjacent to elements with a higher entry pressure, whether the element itself

will be invaded is fully dependent on its neighbours. We call such an element 'locally non-dominant' and its neighbours 'locally dominant' ones, and the trapping pattern will depend only on the order relation of the locally dominant elements. The order relation between pores or between throats is symmetric and does not affect the trapping pattern, and as a result the control parameters need only to capture the order relation between a pore and a throat. We define the local pore-dominance PD_L as the percentage of locally dominant pores among all pores. Here, $PD_L = 0$ and $PD_L = 1$ correspond to site-percolation and bond-percolation, respectively (Stauffer & Aharony 2018). Among the locally dominant elements, we define the non-local pore-dominance PD_N as the probability of a pore with a higher entry pressure than a throat. Thus both PD_L and PD_N range from 0 to1.

It is validated here whether PD_L and PD_N control the trapping patterns by IP. For each set of PD_L and PD_N, at least four distinctively different sets of distributions are adopted, and for each set of distributions, at least 16 spatially different networks are generated. The details of the distributions are explained as follows. Each distribution, either the distribution of the element size or contact angle, is a combination of multiple normal distributions. Each normal distribution has its average value, standard deviation and probability weight, which can all be adjusted to change the values of PD_L and PD_N. In this work, the average value of each normal distribution of the element size ranges from 1 to 2000, the standard deviation ranges from 0 % to 100 % of the corresponding average value, and the probability weight is naturally between 0 and1. The contact angle naturally ranges from 0 to 180°, and we set the deviation to be between 0° and 40°. PD_L and PD_N produced by different sets of distributions are considered to be the same if the standard deviation is smaller than 0.1 %. It is found that the networks with the same PD_L and PD_N have similar trapping percentage (percentage of trapped elements in number) with standard deviation less than 2 % and similar distributions of trapped elements along the sequence of entry pressure. Therefore, for IP in random networks, PD_L and PD_N are the two essential control parameters. This finding is consistent with one previous report, which studied the throat-dominated case, corresponding to $PD_L = 0$ in our work, and found that the residual saturation was invariant of the structure (Chandler *et al.* 1982).

Figure 2 illustrates the average trapping percentage of pores and throats when PD_L and PD_N range from 0 to 1. The results indicate that larger PD_L and PD_N lead to more trapping of pores and less trapping of throats. The overall trapping percentage of elements is high regardless of PD_L and PD_N, namely regardless of the wetting condition, consistent with existing knowledge (Cieplak & Robbins 1988). Figure 3 shows the distribution of trapped elements from four sets of PD_L and PD_N, with elements divided into locally dominant and non-dominant ones. Locally non-dominant elements have a trapping percentage irrelevant to their order relation of entry pressure, as expected. An important feature presented in both figures 2 and 3 is that the trapping percentage is most affected by the portion of elements that are most dominant, namely hardest to invade, and in our results this portion is approximately the higher half in entry pressure of locally dominant elements, one-quarter of all elements. This can be directly observed from the zero slope in figure 2, which indicates that variations of PD_L here do not affect the trapping percentage, because the most dominant quarter of elements is unchanged. The distribution of trapped elements in figure 3 may provide an explanation: half of the locally dominant elements with higher entry pressure are almost fully trapped, while the rest have a considerably lower trapping percentage similar to the locally non-dominant elements. As a result, the overall trapping percentage is mainly determined by the portion fully trapped.

The impact of wettability and structure on trapping can be interpreted from the trapping patterns. Note that in applications, the amount or volume of the trapped oil is the major

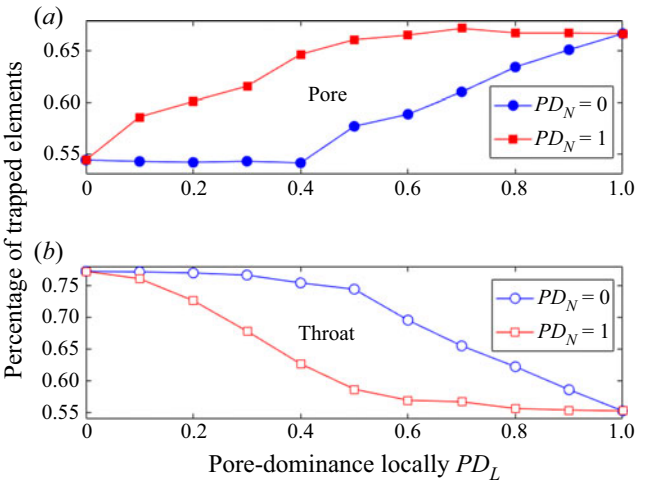

Figure 2. The trapping percentages of pores and throats with varying PD_L and PD_N, calculated by IP. Results are averaged from at least four distinctively different sets of distributions and at least 16 spatially different networks for each set of distributions. The standard deviation is less than2 %.

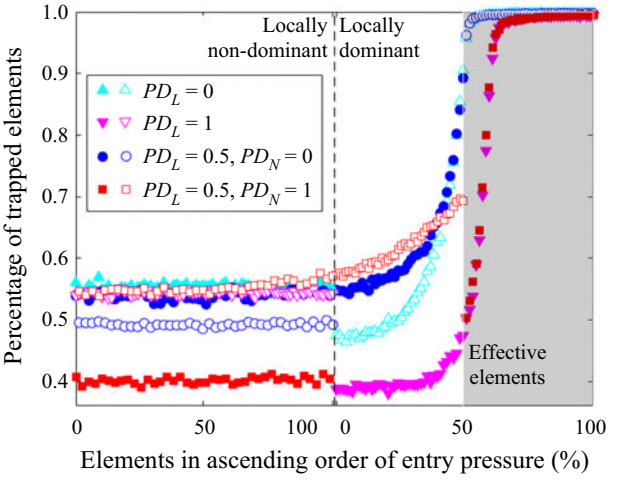

Figure 3. The distribution of trapped elements arranged in the order of entry pressure, with elements divided into locally dominant and non-dominant ones, at four sets of PD_L and PD_N. The filled symbols are pores and unfilled symbols are throats, as in figure 2.

concern, instead of the percentage of trapped elements in number. Quantitatively, PD_L and PD_N can be calculated from given wettability and structures, and the corresponding trapping patterns along with input distributions yield the amount of trapping. We thus obtain a general rule from the feature that the most dominant portion is fully trapped, and that the least trapping condition is 'the most dominant elements having small volume'. Therefore, for the same structure, homogeneous oil-wet is better than homogeneous water-wet because under an oil-wet condition, smaller elements have a higher entry pressure. Similarly, deductions can be made that a water-wet condition favours a homogeneous pore size distribution, while an oil-wet condition favours a heterogeneous one.

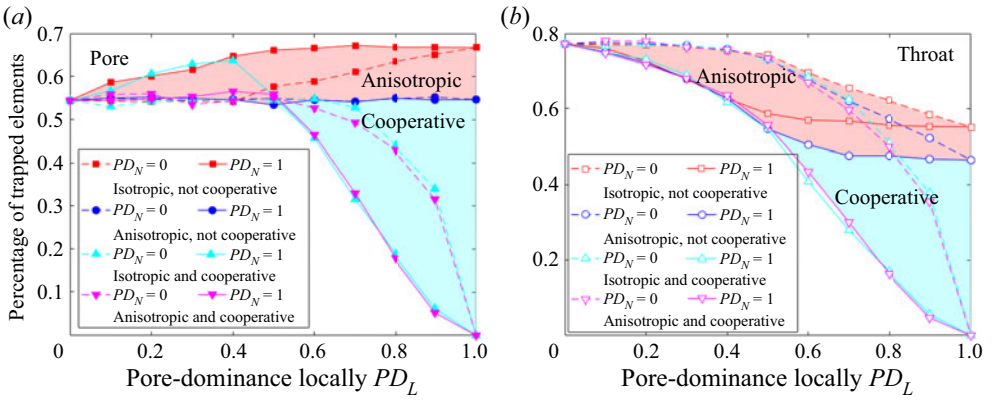

Figure 4. The trapping percentages of pores and throats with all four control parameters varied, calculated by the full model. Similar to figure 2, results are averaged and the standard deviation is small.

The full model with pore filling included is now considered. We propose that pore filling brings two more control parameters compared with IP. The first is the efficacy of anisotropy E_{aniso}. Now a pore can have multiple entry pressures from different directions as the diverging angle varies. Consequently, the order relation involving a pore becomes flexible as a pore may have a higher entry pressure in one direction but a lower one in the other. This should reduce trapping as the flow forward restricts the direction and loses the flexibility, leading to more flat displacing front. Here, E_{aniso} also depends on the heterogeneity of the network, as the order relation is less affected by anisotropy in more heterogeneous cases. The second control parameter is the efficacy of cooperative effect E_{coop}. Cooperative effect is recognized as being capable of reducing trapping, but it contributes only to displacements when the interface is impeded before cooperation and not impeded after. The interface being impeded within a pore requires the primary capillary pressure of this pore to be higher than for adjacent throats, and the secondary capillary pressure of this pore to be higher than the primary one, which means that the pore has to be locally dominant and water-wet. It not being impeded after cooperation requires that the resulting decrease of entry pressure changes the order relation involving this pore, otherwise cooperation will not change the displacing sequence. As a result, the cooperative effect favours homogeneous distribution of capillary pressure. Since the percentage of locally dominant pores is captured by PD_L, E_{coop} can be defined as function of the percentage of water-wet pores among locally dominant ones and the heterogeneity of the network.

Without giving the exact expressions of E_{aniso} and E_{coop}, we can find their upper and lower bounds for fixed PD_L and PD_N. Anisotropy has no efficacy when the range of entry pressures from different directions of one pore never overlaps with that of another pore. In this way there is still a clear order relation of pores. On the contrary, it has the most efficacy when the entry pressures of pores are assigned independently, regardless of which pore they belong to. Cooperative effect has no efficacy when the difference in entry pressure between any two pores is large enough, so that the cooperation does not change the sequence. On the contrary, it has the most efficacy when all locally dominant pores are water-wet and the entry pressures of pores are close, so that the occurrence of cooperative effect always leads to filling of an otherwise impeded pore. Two bounds of these two parameters give four groups, and by varying PD_L and PD_N, the full range of trapping patterns can be obtained in figure 4.

Figure 4 shows the trapping percentages of pores and throats with the four control parameters at their bounds. Similar to figure 2, each point is the average of results from different input distributions. When there is no efficacy of either anisotropy or cooperative effect, the pattern reduces to IP, which validates that E_{aniso} and E_{coop} are the only additional control parameters when pore filling is considered.

Both anisotropy and cooperative effect reduce the amount of trapping and have stronger impact at larger PD_L and PD_N, which agrees with theoretical analyses. The impact of the cooperative effect agrees with previous studies (Blunt 1998; Valvatne & Blunt 2004). The impact of E_{aniso} on pores can be understood as shifting the trapping patterns towards the IP case ($PD_L = 0$). If we increase the entry pressure of a throat to equal that of its connected pore if the entry pressure of the pore is higher and let the pore be locally non-dominant, then the trapping of pores will be the same. Entry pressures of throats connected to the same pore are naturally anisotropic since they are assigned independently. Therefore the most anisotropic cases at any PD_L and PD_N should have the same trapping behaviour of pores as the IP case at $PD_L = 0$, as illustrated in figure 4. A higher E_{aniso} also decreases the trapping of throats because more filled pores means a larger area to be swept. The range of possible trapping with anisotropy introduced is indicated by the red area marked 'Anisotropic' in figure 4: the capability of E_{aniso} for reducing trapping is limited, and the general feature of IP still remains.

Cooperative effect, on the other hand, has the potential to fully eliminate trapping. It removes the IP feature that the most dominant portion of elements determines the trapping percentage, evident from the sharp slope near $PD_L = 1$. In this case, every locally dominant pore decreases the trapping further, regardless of its sequence. It also breaks the rule that higher pore dominance leads to more trapping of pores when E_{coop} is high enough. The light blue area marked 'Cooperative' in figure 4 indicates the range where the cooperative effect must be involved.

Now we consider the cases where both effects are present. The trapping percentage by both effects always overlaps with that by either one alone, which indicates that there is no synergistic effect. Since the capability of anisotropy to decrease trapping is limited, when the cooperative effect is strong at large pore-dominance, it dominates over anisotropy. On the contrary, at a low pore-dominance, introduction of cooperative effect alone does not reduce trapping at all, and the reduced trapping, compared with IP, owes all to anisotropy. When the anisotropy and cooperative effect have a similar impact on reducing trapping independently – for example, at $PD_L = 0.5,\ PD_N = 1$, where the trapping percentages by each effect alone or together all overlap – the anisotropy still dominates over the cooperative effect. It is evident in figure 5 that the distribution of trapped throats is arranged in the order of entry pressure at this point. When both effects are present, the distribution is the same as when only anisotropy is involved, and very different from that where there is only the cooperative effect. We conclude therefore that anisotropy dominates until the cooperative effect leads to less trapping alone.

Here we recapitulate how the four controlling parameters affect the trapping patterns and their relations with wettability and structure in general. The pore-dominance, either PD_L or PD_N, is a description of higher entry capillary pressure of pores compared to throats. Naturally, elements with higher entry pressure are less likely to be displaced. Therefore high pore-dominance leads to more trapping of pores and less trapping of throats. In a perfectly homogeneous wetting condition, due to the diverging angle, pores will always be locally dominant and thus $PD_L = 1$. Homogeneity of the structure will further cause PD_N to be close to 1. Only heterogeneous conditions that lead to relatively low entry pressure of pores can produce lower PD_L and PD_N. Without anisotropy and cooperative

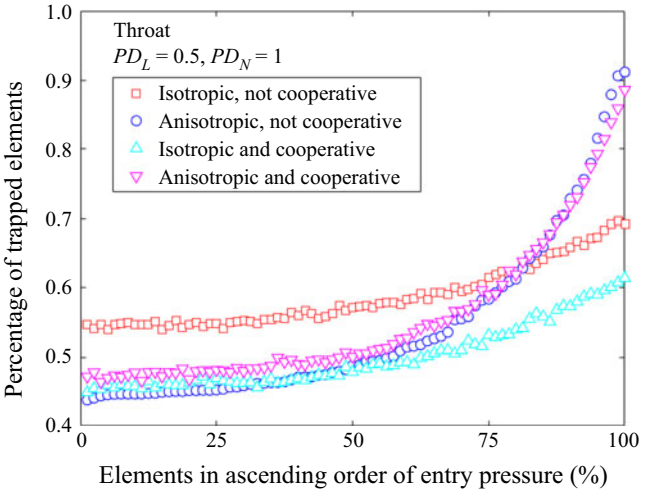

Figure 5. The distribution of trapped throats arranged in the order of entry pressure at $PD_L = 0.5$, $PD_N = 1$, from four combinations of anisotropy and cooperative effect.

effect, the overall trapping percentage will be high regardless, since either pores or throats are dominant and contribute to the trapping. The two other parameters, E_{aniso} and E_{coop}, can reduce trapping in that they can alter the fixed order relation between elements. The anisotropy alters the fixed relation by allowing pores to have different entry pressures from different directions, and the cooperative effect directly changes the entry pressure of pores during displacement. Both of these effects favour homogeneous structure, because if the structure is highly heterogeneous, then the change of entry pressure of one element may not change the order relation between it and another element. For the same reason, both favour high pore-dominance as well since they can affect only the entry pressure of pores. The occurrence of cooperative effects additionally requires the wetting condition to be water-wet.

The impact of various combinations of pore geometry, pore size and wettability distributions on trapping is readily predicted based on numerical simulations. It is especially important that those factors have to be considered together because they influence the control parameters essentially. For example, the water-wet condition together with the homogeneous structure reduce trapping the most, while the water-wet condition alone is not necessarily better than the oil-wet one, and the homogeneous structure is not necessarily better than the heterogeneous one. These results provide a possible explanation of why in the previous studies, the minimum amount of trapping occurred at the water-wet (Akai *et al.* 2019), neutrally wet (Jadhunandan & Morrow 1995) or oil-wet (Zhao, Blunt & Yao 2010) condition.

Although this work considers only one fixed topology, the qualitative conclusion is general because the theoretical analyses do not rely on any specific topology. For the IP case at $PD_L = 0$, one previous study actually validated that the trapping percentage was invariant of the topology being a square, triangle or hexagon (Chandler *et al.* 1982), and we have successfully repeated this finding.

4. Conclusion

In summary, we have found that the trapping pattern of bypassing during capillary displacement is determined by four dimensionless control parameters, PD_L, PD_N, E_{aniso}

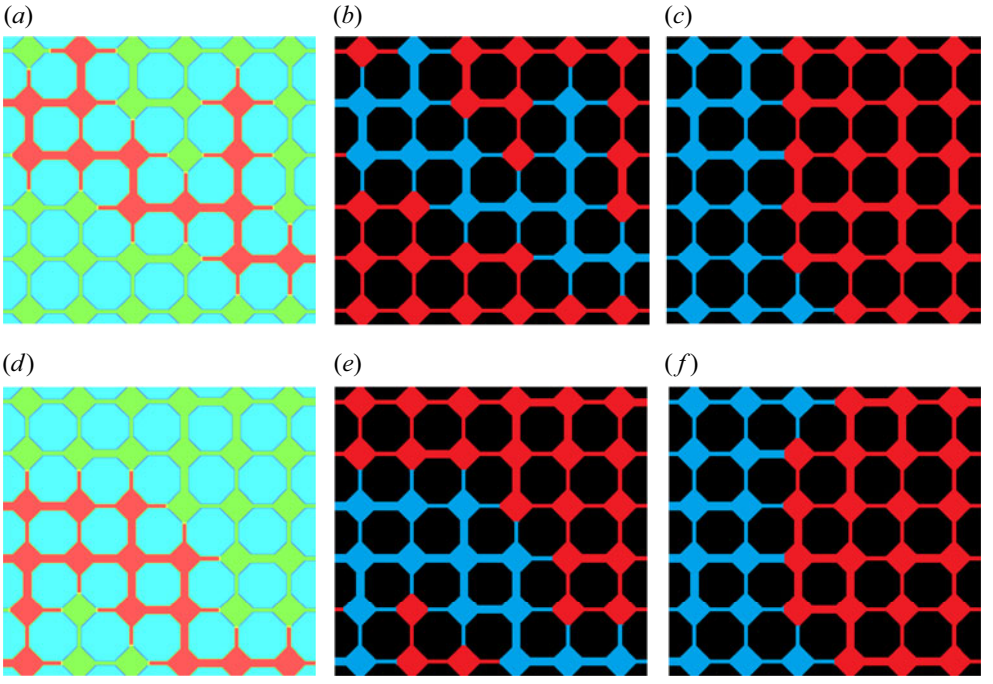

Figure 6. Two-phase distribution obtained by LBM, our algorithm and the traditional pore-network model without considering the diverging angle at pore-throat junctions, for two randomly generated networks. (*a–c*) are results for network 1 and (*d–f*) are results for structure 2. (*a*,*d*) are obtained by LBM, where the red phase is water and the green phase is oil. (*b*,*e*) are obtained by our algorithm, where the red phase is oil and the blue phase is water. (*c*,*f*) are obtained by the traditional pore-network model with the same simulation steps as (*b*,*e*).

and E_{coop}, which can be calculated *a priori* from the wettability distribution, pore size distribution and pore geometry. We have obtained the range of all possible trapping patterns for randomly generated networks, and shown the relation between patterns and control parameters. The results are open to many interpretations in terms of the impact of wettability and structure on trapping.

Funding. This work is funded by the National Key R&D Program of China (no. 2019YFA0708704), NSF grant of China (no. U1837602) and the Tsinghua University Initiative Scientific Research Program for financial support.

Declaration of interests. The authors report no conflict of interest.

Author ORCIDs.
Moran Wang https://orcid.org/0000-0002-0112-5150.

Author contributions. M.W. conceived and promoted this work. F.L. performed the simulations and analysis. F.L. wrote the paper and M.W. revised the text.

Appendix

We validate this algorithm and at the same time show the necessity of introducing the geometrical parameter ϕ by doing a comparison with the two-phase lattice Boltzmann method (LBM), which has been validated in our previous works. The algorithm in this work assumes a capillary-dominated flow, which in reality is achieved by the extremely small flow rate in reservoir conditions. However, in numerical simulations such a small

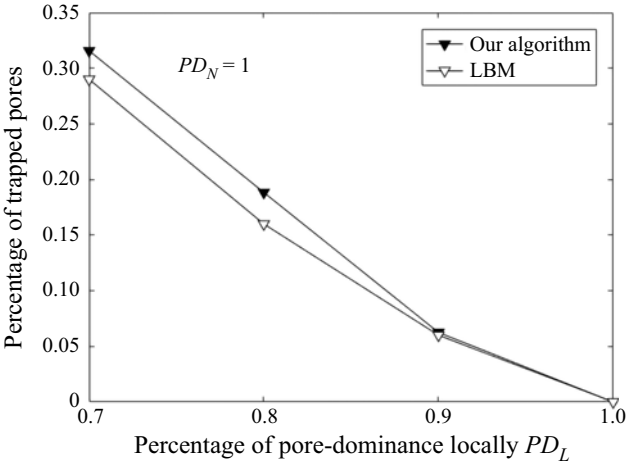

Figure 7. Percentage of trapped pores obtained by our algorithm and LBM, when cooperative effect is important.

flow rate will lead to very long computing times and high computational costs, and we realize the capillary-dominated flow by manually setting higher interfacial tension and lower viscosity. For the same structure and wettability, we compare the two-phase distribution by LBM, our algorithm, and the traditional pore-network model that does not consider the diverging angle ϕ, as shown in figure 6. Exact agreement is achieved between our algorithm and LBM for the two randomly generated structures.

It is possible to do the same comparison for larger structures, but since the stability of LBM has requirements over the viscosity of fluid, maintaining capillary-dominated flow has to be achieved by reducing the inlet velocity. This will increase the computation cost considerably, and we think it is unnecessary as a larger structure does not bring new physics. Also, since we adopt a simple treatment of the coefficients related to cooperative effect, we do not expect exact agreement pore-by-pore when the cooperative effect is important. Instead, we validate that the overall trapping percentage is similar by LBM and our algorithm, even when the efficacy of the cooperative effect is at its upper bound, shown in figure 7. The deviation is because the structure in LBM is not large enough.

References

Akai, T., Alhammadi, A.M., Blunt, M.J. & Bijeljic, B. 2019 Modeling oil recovery in mixed-wet rocks: pore-scale comparison between experiment and simulation. *Transp. Porous Media* **127** (2), 393–414.

Aker, E., Måløy, K.J. & Hansen, A. 2000 Viscous stabilization of 2D drainage displacements with trapping. *Phys. Rev. Lett.* **84** (20), 4589.

Al-Gharbi, M.S. & Blunt, M.J. 2005 Dynamic network modeling of two-phase drainage in porous media. *Phys. Rev.* E **71** (1), 016308.

Avendaño, J., Lima, N., Quevedo, A. & Carvalho, M. 2019 Effect of surface wettability on immiscible displacement in a microfluidic porous media. *Energies* **12** (4), 664.

Berg, S., Cense, A.W., Jansen, E. & Bakker, K. 2010 Direct experimental evidence of wettability modification by low salinity. *Petrophysics* **51** (5), 314–322.

Berg, S. & Ott, H. 2012 Stability of CO2–brine immiscible displacement. *Intl J. Greenh. Gas Control* **11**, 188–203.

Blunt, M.J. 1998 Physically-based network modeling of multiphase flow in intermediate-wet porous media. *J. Petrol. Sci. Engng* **20** (3–4), 117–125.

BLUNT, M.J. 2017 *Multiphase Flow in Permeable Media: A Pore-scale Perspective*. Cambridge University Press.

CHANDLER, R., KOPLIK, J., LERMAN, K. & WILLEMSEN, J.F. 1982 Capillary displacement and percolation in porous media. *J. Fluid Mech.* **119**, 249–267.

CHEN, J.-D. & WILKINSON, D. 1985 Pore-scale viscous fingering in porous media. *Phys. Rev. Lett.* **55** (18), 1892.

CIEPLAK, M. & ROBBINS, M.O. 1988 Dynamical transition in quasistatic fluid invasion in porous media. *Phys. Rev. Lett.* **60** (20), 2042.

ESMAEILZADEH, S., QIN, Z., RIAZ, A. & TCHELEPI, H.A. 2020 Wettability and capillary effects: dynamics of pinch-off in unconstricted straight capillary tubes. *Phys. Rev.* E **102** (2), 023109.

GU, Q., LIU, H. & WU, L. 2021 Preferential imbibition in a dual-permeability pore network. *J. Fluid Mech.* **915**, A138.

HOLTZMAN, R. & SEGRE, E. 2015 Wettability stabilizes fluid invasion into porous media via nonlocal, cooperative pore filling. *Phys. Rev. Lett.* **115** (16), 164501.

HUPPERT, H.E. & NEUFELD, J.A. 2014 The fluid mechanics of carbon dioxide sequestration. *Annu. Rev. Fluid Mech.* **46**, 255–272.

JADHUNANDAN, P.P. & MORROW, N.R. 1995 Effect of wettability on waterflood recovery for crude-oil/brine/rock systems. *SPE Res. Engng* **10** (1), 40–46.

LENORMAND, R., TOUBOUL, E. & ZARCONE, C. 1988 Numerical models and experiments on immiscible displacements in porous media. *J. Fluid Mech.* **189** (1), 165–187.

LENORMAND, R. & ZARCONE, C. 1985 Invasion percolation in an etched network: measurement of a fractal dimension. *Phys. Rev. Lett.* **54** (20), 2226.

LIU, F. & WANG, M. 2020 Review of low salinity waterflooding mechanisms: wettability alteration and its impact on oil recovery. *Fuel* **267**, 117112.

MÅLØY, K.J., FEDER, J. & JØSSANG, T. 1985 Viscous fingering fractals in porous media. *Phys. Rev. Lett.* **55** (24), 2688.

ODIER, C., LEVACHÉ, B., SANTANACH-CARRERAS, E. & BARTOLO, D. 2017 Forced imbibition in porous media: a fourfold scenario. *Phys. Rev. Lett.* **119** (20), 208005.

PAYATAKES, A.C. 1982 Dynamics of oil ganglia during immiscible displacement in water-wet porous media. *Annu. Rev. Fluid Mech.* **14** (1), 365–393.

RABBANI, H.S., OR, D., LIU, Y., LAI, C.-Y., LU, N.B., DATTA, S.S., STONE, H.A. & SHOKRI, N. 2018 Suppressing viscous fingering in structured porous media. *Proc. Natl Acad. Sci. USA* **115** (19), 4833–4838.

RAEINI, A.Q., BIJELJIC, B. & BLUNT, M.J. 2018 Generalized network modeling of capillary-dominated two-phase flow. *Phys. Rev.* E **97** (2), 023308.

RÜCKER, M., BERG, S., ARMSTRONG, R.T., GEORGIADIS, A., OTT, H., SCHWING, A., NEITELER, R., BRUSSEE, N., MAKURAT, A. & LEU, L. 2015 From connected pathway flow to ganglion dynamics. *Geophys. Res. Lett.* **42** (10), 3888–3894.

SAHINI, M. & SAHIMI, M. 2003 *Applications of Percolation Theory*. CRC Press.

SHEPPARD, A.P., KNACKSTEDT, M.A., PINCZEWSKI, W.V. & SAHIMI, M. 1999 Invasion percolation: new algorithms and universality classes. *J. Phys.* A*: Math. Gen.* **32** (49), L521.

SINGH, K., JUNG, M., BRINKMANN, M. & SEEMANN, R. 2019 Capillary-dominated fluid displacement in porous media. *Annu. Rev. Fluid Mech.* **51**, 429–449.

STAUFFER, D. & AHARONY, A. 2018 *Introduction to Percolation Theory*. CRC Press.

TAHERIOTAGHSARA, M., BONTO, M., EFTEKHARI, A.A. & NICK, H.M. 2020 Prediction of oil breakthrough time in modified salinity water flooding in carbonate cores. *Fuel* **274**, 117806.

TRAN, T.Q., NEOGI, P. & BAI, B. 2017 Stability of CO_2 displacement of an immiscible heavy oil in a reservoir. *SPE J.* **22** (2), 539–547.

TROJER, M., SZULCZEWSKI, M.L. & JUANES, R. 2015 Stabilizing fluid-fluid displacements in porous media through wettability alteration. *Phys. Rev. Appl.* **3** (5), 054008.

TSUJI, T., JIANG, F. & CHRISTENSEN, K.T. 2016 Characterization of immiscible fluid displacement processes with various capillary numbers and viscosity ratios in 3D natural sandstone. *Adv. Water Resour.* **95**, 3–15.

VALVATNE, P.H. & BLUNT, M.J. 2004 Predictive pore-scale modeling of two-phase flow in mixed wet media. *Water Resour. Res.* **40** (7), W07406.

VISHNUDAS, R. & CHAUDHURI, A. 2017 A comprehensive numerical study of immiscible and miscible viscous fingers during chemical enhanced oil recovery. *Fuel* **194**, 480–490.

WANG, Z., CHAUHAN, K., PEREIRA, J.-M. & GAN, Y. 2019 Disorder characterization of porous media and its effect on fluid displacement. *Phys. Rev. Fluids* **4** (3), 034305.

WANG, Z., PEREIRA, J.-M. & GAN, Y. 2020 Effect of wetting transition during multiphase displacement in porous media. *Langmuir* **36** (9), 2449–2458.

WANG, Z., PEREIRA, J.-M. & GAN, Y. 2021 Effect of grain shape on quasi-static fluid-fluid displacement in porous media. *Water Resour. Res.* **57** (4), e2020WR029415.

WILKINSON, D. & WILLEMSEN, J.F. 1983 Invasion percolation: a new form of percolation theory. *J. Phys.* A*: Math. Gen.* **16** (14), 3365.

ZHAO, B., MACMINN, C.W. & JUANES, R. 2016 Wettability control on multiphase flow in patterned microfluidics. *Proc. Natl Acad. Sci. USA* **113** (37), 10251–10256.

ZHAO, B., MACMINN, C.W., PRIMKULOV, B.K., CHEN, Y., VALOCCHI, A.J., ZHAO, J., KANG, Q., BRUNING, K., MCCLURE, J.E. & MILLER, C.T. 2019 Comprehensive comparison of pore-scale models for multiphase flow in porous media. *Proc. Natl Acad. Sci. USA* **116** (28), 13799–13806.

ZHAO, X., BLUNT, M.J. & YAO, J. 2010 Pore-scale modeling: effects of wettability on waterflood oil recovery. *J. Petrol. Sci. Engng* **71** (3–4), 169–178.